
PHYSICAL ORGANOMETALLIC
CHEMISTRY VOLUME 4

Fluxional Organometallic and Coordination Compounds

Edited by

MARCEL GIELEN

Free University of Brussels, Belgium

RUDOLPH WILLEM

Free University of Brussels, Belgium

BERND WRACKMEYER

Universität Bayreuth, Germany



John Wiley & Sons, Ltd

Fluxional Organometallic and Coordination Compounds

Physical Organometallic Chemistry

Editorial Board

Marcel Gielen, Free University of Brussels, Belgium

Rudolph Willem, Free University of Brussels, Belgium

Bernd Wrackmeyer, Universität Bayreuth, Germany

Books previously published in this Series

Volume 1 Advance Applications of NMR to Organometallic Chemistry

Edited by

Marcel Gielen, Free University of Brussels, Belgium

Rudolph Willem, Free University of Brussels, Belgium

Bernd Wrackmeyer, Universität Bayreuth, Germany

ISBN 0 471 95938 3

Volume 2 Solid State Organometallic Chemistry

Edited by

Marcel Gielen, Free University of Brussels, Belgium

Rudolph Willem, Free University of Brussels, Belgium

Bernd Wrackmeyer, Universität Bayreuth, Germany

ISBN 0 471 97920 1

Volume 3 Unusual Structures and Physical Properties in Organometallic Chemistry

Edited by

Marcel Gielen, Free University of Brussels, Belgium

Rudolph Willem, Free University of Brussels, Belgium

Bernd Wrackmeyer, Universität Bayreuth, Germany

ISBN 0 471 49635 9

PHYSICAL ORGANOMETALLIC
CHEMISTRY VOLUME 4

Fluxional Organometallic and Coordination Compounds

Edited by

MARCEL GIELEN

Free University of Brussels, Belgium

RUDOLPH WILLEM

Free University of Brussels, Belgium

BERND WRACKMEYER

Universität Bayreuth, Germany



John Wiley & Sons, Ltd

Copyright © 2004 John Wiley & Sons Ltd, The Atrium, Southern Gate, Chichester,
West Sussex PO19 8SQ, England

Telephone (+44) 1243 779777

Email (for orders and customer service enquiries): cs-books@wiley.co.uk
Visit our Home Page on www.wileyeurope.com or www.wiley.com

All Rights Reserved. No part of this publication may be reproduced, stored in a retrieval system or transmitted in any form or by any means, electronic, mechanical, photocopying, recording, scanning or otherwise, except under the terms of the Copyright, Designs and Patents Act 1988 or under the terms of a licence issued by the Copyright Licensing Agency Ltd, 90 Tottenham Court Road, London W1T 4LP, UK, without the permission in writing of the Publisher. Requests to the Publisher should be addressed to the Permissions Department, John Wiley & Sons Ltd, The Atrium, Southern Gate, Chichester, West Sussex PO19 8SQ, England, or emailed to permreq@wiley.co.uk, or faxed to (+44) 1243 770620.

This publication is designed to provide accurate and authoritative information in regard to the subject matter covered. It is sold on the understanding that the Publisher is not engaged in rendering professional services. If professional advice or other expert assistance is required, the services of a competent professional should be sought.

Other Wiley Editorial Offices

John Wiley & Sons Inc., 111 River Street, Hoboken, NJ 07030, USA

Jossey-Bass, 989 Market Street, San Francisco, CA 94103-1741, USA

Wiley-VCH Verlag GmbH, Boschstr. 12, D-69469 Weinheim, Germany

John Wiley & Sons Australia Ltd, 33 Park Road, Milton, Queensland 4064, Australia

John Wiley & Sons (Asia) Pte Ltd, 2 Clementi Loop #02-01, Jin Xing Distripark, Singapore 129809

John Wiley & Sons Canada Ltd, 22 Worcester Road, Etobicoke, Ontario, Canada M9W 1L1

Wiley also publishes its books in a variety of electronic formats. Some content that appears in print may not be available in electronic books.

Library of Congress Cataloging-in-Publication Data

Fluxional organometallic and coordination compounds / edited by Marcel Gielen, Rudolph Willem, Bernd Wrackmeyer.

p. cm. – (Physical organometallic chemistry : v. 4)

Includes bibliographical references and index.

ISBN 0-470-85839-7 (cloth : alk. paper)

1. Coordination compounds. 2. Organometallic chemistry. 3. Molecular dynamics.
4. Nuclear magnetic resonance spectroscopy. I. Gielen, M. (Marcel), 1938- II. Willem, R. (Rudolf)
III. Wrackmeyer, Bernd, 1947- IV. Series.

QD411.F58 2004

541'.2242-dc22

2004003666

British Library Cataloguing in Publication Data

A catalogue record for this book is available from the British Library

ISBN 0 470 85839 7

Typeset in 10.5/12pt Times New Roman by TechBooks, New Delhi, India

Printed and bound in Great Britain by MPG, Bodmin, Cornwall

This book is printed on acid-free paper responsibly manufactured from sustainable forestry in which at least two trees are planted for each one used for paper production.

Contents

Contributors	xi
Series Preface	xiii
Preface	xv
1 Polyhedral Dynamics and the Jahn–Teller Effect	
<i>R. Bruce King</i>	
1 Introduction	1
2 Polyhedron Topology	2
3 Polyhedral Isomerizations: Microscopic Models	6
3.1 Diamond–Square–Diamond Processes	6
3.2 Gale Diagrams	11
3.3 Generation of Metallaborane Structures by Diamond–Square–Diamond Transformations in Deltahedra	18
4 Polyhedral Isomerizations: Macroscopic Models	21
4.1 Topological Representations of Polyhedral Isomerizations	21
4.2 Topological Representations of Jahn–Teller Distortions	28
5 Acknowledgement	37
6 References	37
2 NMR Studies of Intramolecular Dynamics in Allylic Type Triorganoboranes	
<i>I. D. Gridnev and O. L. Tok</i>	
1 Introduction	41
2 Discovery Activation Parameters of [1,3]-B Shifts	42
3 Fluxional Linear Polyunsaturated Allylboranes	47
3.1 2,4-Pentadienyl(di- <i>n</i> -propyl)borane	47
3.2 2,4,6-Heptatrienyl(di- <i>n</i> -propyl)borane	50
4 Dynamic Behavior of Cyclic Allylboranes	53
4.1 Dynamic Equilibria Between 2-(Dialkylboryl)methylenecyclobutanes and 1-(Dialkylboryl)cyclobutenes	53
4.2 Dynamic Properties of Cyclopentadienyl and Pentamethylcyclopentadienyl Derivatives of Boron	58
4.3 Synthesis and Dynamic Properties of 1-Indenyl(diethyl)borane	58

4.4	Dynamic Behavior of Cycloheptadienyl(di- <i>n</i> -propyl) borane	60
4.5	Synthesis and Dynamic Properties of Cycloheptatrienyl(di- <i>n</i> -propyl)borane. Equilibrium with 7-(Di- <i>n</i> -propylboryl)norcaradiene	61
4.6	Three Independent Dynamic Processes in the Irontricarbonyl Complex of Cycloheptatrienyl(di- <i>n</i> -propyl)borane	65
4.7	Cyclooctatetraenyl(di- <i>n</i> -propyl)borane	67
4.8	Sigmatropic Migrations and Thermal Rearrangements in Cyclononatetraenyl(di- <i>n</i> -propyl)borane. Comparison with the Dynamic Properties of Cyclononatetraenyl(trimethyl)tin	70
4.9	Borotropic Migrations in Phenalenyl(di- <i>n</i> -propyl)borane 24	75
5	Diverse Chemoselectivity of Cyclic Polyunsaturated Organoboranes	77
5.1	Chemical Behavior of Borane 23	77
5.2	Diverse Chemoselectivity of 9-Cyclopentyl-9-borababaralane 54e	79
6	Conclusion	81
7	References	81

3 Dynamic Behavior of Group 5 and 6 Transition Metal Complexes with NMR

S. Sakharov

1	Introduction	85
2	Rotational Isomerism in Amido and Ketimido Complexes	86
2.1	Rotational Isomerism in Oxofluoramido Complexes of Tungsten(VI)	86
2.2	Restricted M–NR ₂ Rotation in the Dinuclear Complexes with M ₂ ⁶⁺ Core (M = W, Mo)	91
2.3	Features of Dynamic Behavior of Amido Cyclopentadienyl Complexes of Group 5 Transition Metals	93
2.4	Internal Hindered Rotation of Ketimido Ligands	95
3	Dynamic Behavior of d ⁰ Transition Metal Complexes with n-Donor Two-Center Ligands	98
3.1	Isomerization of Fluorocomplexes of Group 5–6 with O, N-Two-Center Ligands	98
3.2	Isomerism of Transition Metal Complexes with N, N-Two-center Ligands	110
3.3	Nature of Bonding of n-Donor Two-center Ligands in d ⁰ Transition Metal Complexes	119
3.4	Mechanism of Internal Hindered Rotation of η ² -Bound Ligands	121
4	Conclusion	126
5	References	126

4 Conformational Mobility in Chelated Square-planar Rh, Ir, Pd, and Pt Complexes

P. Espinet and J. A. Casares

1	Introduction	131
2	Conformational Changes in Five-member Metallacycles	132
3	Conformational Changes in Six-member Metallacycles	142
4	Conformational Changes in Five- or Six-member Metallacycles Involving Coordinated Olefins	152
5	Conformational Changes in Seven-member Metallacycles	154
6	Conformational Changes in Higher Metallacycles	156
7	Acknowledgment	158
8	References	158

5 Dynamic and Kinetic Aspects of Metallodrugs by NMR

F. Li and H. Sun

1	Introduction	163
2	Methods of Study by NMR	164
3	Platinum Anticancer Drugs	169
3.1	^{195}Pt , ^{15}N and Inverse [^1H , ^{15}N] NMR Spectroscopy	170
3.2	Activation of Platinum Anticancer Drugs: Kinetics and Equilibria of Aquation	173
3.3	Platination of Nucleotides and DNA	176
3.4	Interaction of Platinum Agents with Amino Acids, Peptides and Proteins	182
4	Titanium and Ruthenium Anticancer Agents	185
5	Gold Antiarthritic Drugs	188
6	Antimony Antiparasitic and Bismuth Antiulcer Drugs	193
7	Vanadium Antidiabetic Mimetics	197
8	MRI Contrast Agents	202
9	Concluding Remarks	209
10	Abbreviations	209
11	Acknowledgements	210
12	References	210

6 Dynamics by EPR: Picosecond to Microsecond Time Scales

S. Van Doorslaer and G. Jeschke

1	Introduction	219
2	Scope of EPR Spectroscopy	221
2.1	Native Paramagnetic Centers	221
2.2	Spin Labels and Spin Probes	222
3	A Brief Primer on EPR Spectroscopy	223
3.1	Interactions of Electron Spins with Their Environment	223
3.2	Relaxation	226
3.3	Measurement Techniques	227

4	Detection of Dynamic Processes by EPR	229
4.1	Slow Tumbling	229
4.2	Exchange Processes	231
4.3	Dynamic Jahn–Teller Effect	231
4.4	Chemically Induced Dynamic Electron Polarization (CIDEP)	234
5	Application Example: How to Combine Different EPR Techniques	236
6	Acknowledgements	240
7	References	240
7	μSR Studies of Molecular Dynamics in Organometallics <i>U. A. Jayasooriya</i>	
1	Introduction	243
2	Muon	243
3	Muon in Matter	244
4	Experiment	246
5	Muon in a Longitudinal Magnetic Field	247
6	Muon–Electron (Muonium Like) System	250
7	Molecular Dynamics	251
8	Studies of Organometallics	252
8.1	Tetraphenyl Metals	252
8.2	Benzene Chromium Tricarbonyl	252
8.3	Cyclopentadienyl Manganese Tricarbonyl	255
8.4	Ruthenocene	256
8.5	Ferrocene	256
8.6	Ferrocene Encapsulated in Zeolite	261
9	Conclusion	263
9	Acknowledgements	264
10	References	264
8	Proton Dynamics in Solids: Vibrational Spectroscopy with Neutrons <i>F. Fillaux</i>	
1	Introduction	267
2	Vibrational Spectroscopy Techniques	269
2.1	Some Definitions	269
2.2	Optical Techniques	270
2.3	Neutron Scattering Techniques	271
2.4	Potassium Hydrogen Bistrifluoroacetate	276
3	Vibrational Dynamics of Protons in Solids	278
3.1	Force-Field Calculations: Normal versus Localized Modes	278
3.2	The Proton Crystal Model	280

4	Tunnelling	282
4.1	Proton Transfer	282
4.2	Rotational Tunnelling	285
5	Conclusions	301
6	References	302
	Index	305

Contributors

R Bruce King, Department of Chemistry, University of Georgia, Athens, Georgia 30602, USA

Ilya D Gridnev, COE Laboratory, Department of Chemistry, Graduate School of Science, Tohoku University, Sendai 980-8578, Japan

Oleg L Tok, Anorganische Chemie II, University of Bayreuth, D-95440 Bayreuth, Germany

Sergei G Sakharov, Kurnakov Institute of General and Inorganic Chemistry, Russian Academy of Sciences, Leninskii pr. 31, Moscow 119991, Russia

Pablo Espinet, Departamento de Química Inorgánica, Universidad de Valladolid, E- 47005 Valladolid, Spain

Juan A Casares, Departamento de Química Inorgánica, Universidad de Valladolid, E- 47005 Valladolid, Spain

Hongzhe Sun, Department of Chemistry and Open Laboratory of Chemical Biology, University of Hong Kong, Pokfulam Road, Hong Kong

Fei Li, Department of Chemistry and Open Laboratory of Chemical Biology, University of Hong Kong, Pokfulam Road, Hong Kong

Sabine Van Doorslaer, SIBAC Laboratorium, Universiteit Antwerpen – Department Natuurkunde, Universiteitsplein 1, B-2610 Wilrijk, Belgium

Gunnar Jeschke, Max-Planck-Institute for Polymer Research, Postfach 3148, D-55021 Mainz, Germany

Upali Jayasooriya, School of Chemical Sciences, University of East Anglia, Norwich, UK

Françoise Fillaux, Laboratoire de Spectrochimie Infrarouge et Raman, CNRS, 2 rue Henry Dunant, Thiais, France

Series Preface

Physical organic chemistry, the study of the basic physical principles of organic reactions, is not a new field: in 1940, Hammett had already written a book with this title. This area has developed during the last 20 years mainly because of the explosive growth of sophisticated analytical instrumentation and computational techniques, going from the simple Hückel molecular orbital theory to *ab initio* calculations of increasing accuracy enabled by the advent of fast supercomputers.

An analogous genesis characterized physical organometallic chemistry. Understanding the basis of chemical reactivity and the detailed pathways of reactions of organometallic compounds is now one of the major goals of physical organometallic chemists. Correlation of structure with reactivity, increasing in sophistication, contributes powerfully to the understanding of electronic transmission, as well as of steric and conformational properties, including solvent effects. Homogeneous catalysis has reached a development stage making it a wide, complex topic deserving special consideration. Chiral induction is also becoming increasingly important, considering the economic importance of asymmetric syntheses in the design of pharmaceuticals: organometallic compounds play a key role in this area; understanding this role is the key to further progress.

Accordingly, the major developments of physical organometallic chemistry are not only relevant to *ab initio* calculations of metal-based organic compounds or new spectroscopic tools like multidimensional high-resolution NMR. They also involve new ingenious technologies to study reaction mechanisms, group-theoretical approaches to investigate the fluxionality of organometallic molecules, photochemical reactions on organometallic substrates, and, last but not least, experimental highlights like unstable organometallic compounds in matrices, piezochemistry, and sonochemistry.

The main goal of this series 'Physical Organometallic Chemistry' is to offer to post-graduates and researchers leading contributions written by well-known scientists reviewing the state-of-the-art of hot topics animating this wide research area, in order to develop new insights and to promote novel interest and investigations.

Preface

Dynamic processes are of prime importance in all fields of chemistry in order to understand structure and reactivity. With the ever-increasing performance of analytical tools both slow and fast dynamics can be studied and analyzed nowadays to reveal properties of matter which previously have not been fully understood and sometimes not even anticipated. Frequently, we find situations where theory is ahead of experiment, but there are also numerous experimental results which await theoretical explanation. Indeed, fluxional processes taking place in molecules can be determined and explained on various levels of experiment and theory. It is therefore important to be aware of different concepts and techniques, and to look out for the methodologies and research strategies which are most appropriate to tackle dynamic problems. Certainly, this fascinating complex and broad field cannot be covered completely in this book. The topics selected here address some key concepts and methods which may be regarded as useful examples of an interdisciplinary approach. This volume starts off with the dynamic behavior of polyhedral compounds in the light of the Jahn–Teller effect. The first chapter has a general bearing for clusters containing main group elements and/or transition metals. Then, the application of NMR spectroscopy to dynamics is addressed, a field which is very familiar to most people working in organometallic and coordination chemistry. This general topic is treated in many text books and has been reviewed regularly. Therefore, we have picked out examples for a few classes of compounds, and by this we expect that stimulating information is provided to initiate studies in related areas. Allylic boranes open the view into a fascinating world of dynamic behavior of organic compounds when an apparently innocent heteroatom like boron, the neighbor of carbon in the Periodic Table, is present. Transition metal complexes can be regarded as an Eldorado of fluxionality, and representative examples of Groups 5 and 6 and of the platinum metals of Groups 9 and 10 serve to illustrate this point. The origin of dynamics can be sought in the ligands, in the electronic structure of the metal center, or in synergetic effects arising from both ligand and metal. This topic is further elaborated by an excursion to metallo drugs, where the structure–reactivity relationship plays a really vital role. We have left out solid-state NMR in this volume, since dynamic aspects seen by solid-state NMR have been discussed in previous volumes of this series. This is also true for dynamics in single crystals studied by X-ray diffraction analysis. Some people may miss the dynamic behavior of paramagnetic compounds, studied by NMR. Considering the recent monograph (I. Bertini, C. Luchinat,

G. Parigi, *Solution NMR of Paramagnetic Molecules*, Elsevier, Amsterdam, 2001), we decided not to include this subject. Since paramagnetic samples are readily studied by EPR, a relevant chapter provides information on application of EPR to fluxionality. This is not only meant as a report; it also intends to stimulate potential applications in organometallic chemistry. A sufficient muon flux generation requires an appropriate particle accelerator, and therefore, μ -SR spectroscopy (here SR stands for spin relaxation) is rarely applied to investigate fluxionality in organometallic compounds. However, this technique has considerable potential, and it reveals information complementary to other methods, and also shows unexpected new features, where the unpaired electron is playing an active role. The final chapter deals with inelastic neutron scattering (INS) aiming at the study of proton dynamics in solids. The dynamic properties of hydrogen bridges, the behavior of rotors containing hydrogen atoms, starting with the famous dihydrogen ligand in transition metal complexes, followed by the ammonia molecule in various surroundings, and by methyl groups can be analyzed by INS to give a completely new insight into these processes. It can be envisaged that this technique will be applicable to other systems which show pronounced proton fluxionality such as metal hydroborates, metal fluoride complexes, e.g. with M-F...H-F bridges, and to numerous compounds which possess so-called weak hydrogen bridges as in metal hydride complexes with M-H...H-N or M-H...H-C bridges.

1 Polyhedral Dynamics and the Jahn–Teller Effect

R. BRUCE KING

Department of Chemistry, University of Georgia, Athens, GA 30602, USA

1 INTRODUCTION

The role of polyhedra in the static description of chemical structures makes of considerable interest their dynamic properties. In this connection the central concept in the study of polyhedral dynamics is that of a polyhedral isomerization. In this context a polyhedral isomerization is defined as a deformation of a specific polyhedron \mathcal{P}_1 until its vertices define a new polyhedron \mathcal{P}_2 . Of particular interest are sequences of two polyhedral isomerization steps $\mathcal{P}_1 \rightarrow \mathcal{P}_2 \rightarrow \mathcal{P}_3$ in which the final polyhedron \mathcal{P}_3 is combinatorially equivalent to the initial polyhedron \mathcal{P}_1 although with some permutation of the vertices. Such polyhedral isomerization sequences are called degenerate polyhedral isomerizations.

Polyhedral isomerizations may be studied using either a microscopic or macroscopic approach. The microscopic approach uses details of polyhedral topology to elucidate possible single polyhedral isomerization steps, namely which types of isomerization steps are possible. Such isomerization steps consist most commonly of so-called diamond–square–diamond processes or portions thereof. The microscopic approach to polyhedral isomerizations is relevant to understanding fluxional processes in borane and metallaborane polyhedra.

The earliest work on polyhedral isomerizations by Muetterties [1–4], Gielen [5–12], Musher [13,14], Klemperer [15–17] and Brocas [18,19] used a macroscopic approach involving relationships between different permutational isomers. Such relationships may be depicted by reaction graphs called topological representations (or top-reps) in which the vertices correspond to different permutational isomers and the edges correspond to single degenerate polyhedral isomerization steps. The macroscopic point of view is also useful for the classification of Jahn–Teller distortions of polyhedra [20] relating to the instability of a non-linear symmetrical nuclear configuration in an electronic degenerate state [21–24].

Both approaches will be reviewed in this chapter, which expands and updates reviews published by the author in 1988 [25] and 1994 [26] and a book in 1992 [27].

2 POLYHEDRON TOPOLOGY

Before considering polyhedral dynamics it is first necessary to consider the static topology of polyhedra. Of fundamental importance are relationships between possible numbers and types of vertices (v), edges (e), and faces (f) of polyhedra. In this connection the following elementary relationships are particularly significant [28]:

1. Euler's relationship:

$$v - e + f = 2 \quad (1.1)$$

This theorem is illustrated by the five regular polyhedra depicted in Figure 1.1.

2. Relationship between the edges and faces:

$$\sum_{i=3}^{v-1} i f_i = 2e \quad (1.2)$$

In Equation (1.2) f_i is the number of faces with i edges (i.e., f_3 is the number of triangular faces, f_4 is the number of quadrilateral faces, etc.). This relationship arises from the fact that exactly two faces share each edge of the polyhedron. Since no face can have fewer edges than the three of a triangle, the following inequality must hold in all cases:

$$3f \leq 2e \quad (1.3)$$

3. Relationship between the edges and vertices:

$$\sum_{i=3}^{v-1} i v_i = 2e \quad (1.4)$$

In Equation (1.4) v_i is the number of vertices of *degree* i (i.e., having i edges meeting at the vertex in question). This relationship arises from the fact that each edge of the polyhedron connects exactly two vertices. Since no vertex of a polyhedron can have a degree less than three, the following inequality must hold in all cases:

$$3v \leq 2e \quad (1.5)$$

4. Totality of faces:

$$\sum_{i=3}^{v-1} f_i = f \quad (1.6)$$

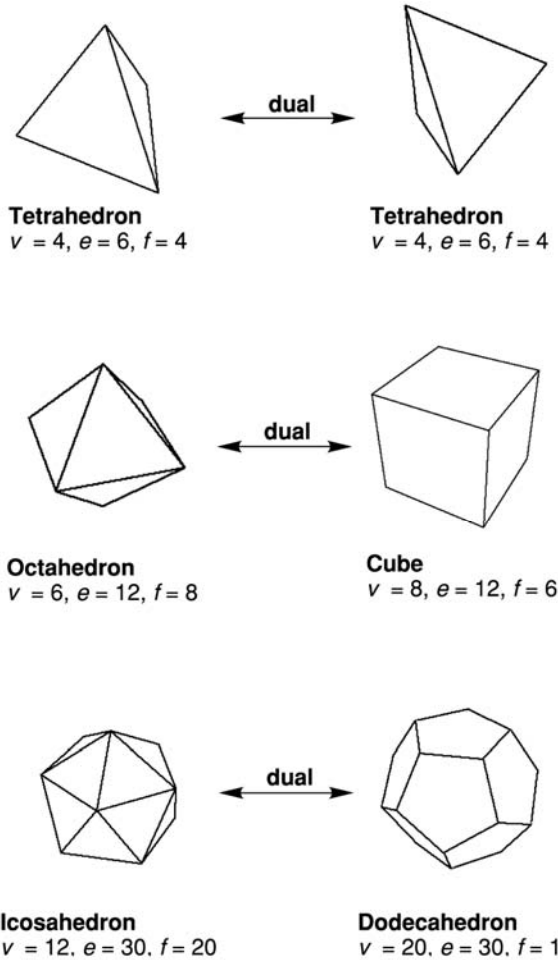


Figure 1.1 The five regular polyhedra depicted as dual pairs.

5. Totality of vertices:

$$\sum_{i=3}^{v-1} v_i = v \quad (1.7)$$

Equation (1.6) relates the f_i s to f and Equation (1.7) relates the v_i s to v .

In generating actual polyhedra, the operations of capping and dualization are often important. *Capping* a polyhedron \mathcal{P}_1 consists of adding a new vertex above the center of one of its faces \mathcal{F}_1 followed by adding edges to connect the new vertex with each vertex of \mathcal{F}_1 . If \mathcal{F}_1 has k edges, then the capping process can be more specifically described as k -capping.

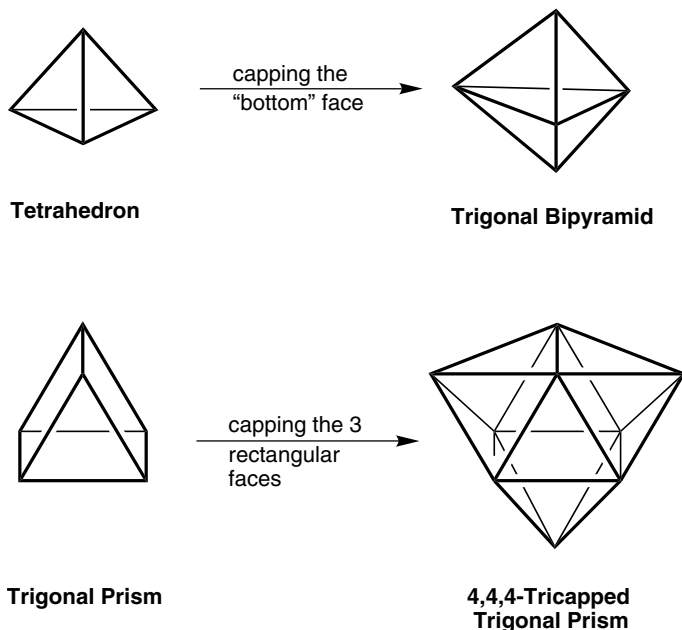


Figure 1.2 (a) Capping a face of the tetrahedron to form a trigonal bipyramid. (b) Capping all three rectangular faces of a trigonal prism to form a D_{3h} tricapped trigonal prism.

The capping process gives a new polyhedron \mathcal{P}_2 having one more vertex than \mathcal{P}_1 . If a triangular face is capped (i.e., 3-capping), the following relationships will be satisfied in which the subscripts 1 and 2 refer to \mathcal{P}_1 and \mathcal{P}_2 , respectively:

$$v_2 = v_1 + 1; \quad e_2 = e_1 + 3; \quad f_2 = f_1 + 2 \quad (1.8)$$

Such a capping of a triangular face is found in the capping of a tetrahedron to form a trigonal bipyramid (Figure 1.2a). In general if a face with f_k edges is capped (i.e., k -capping), the following relationships will be satisfied:

$$v_2 = v_1 + 1; \quad e_2 = e_1 + f_k; \quad f_2 = f_1 + f_k - 1 \quad (1.9)$$

For example, application of such a capping process to each of the three rectangular faces of a trigonal prism generates the 4,4,4-tricapped trigonal prism (Figure 1.2b). This nine-vertex deltahedron appears in both coordination chemistry (e.g., ReH_9^{2-}) and borane chemistry (e.g., $\text{B}_9\text{H}_9^{2-}$).

Another process of interest in polyhedral topology is the *dualization* of polyhedra. A given polyhedron \mathcal{P} can be converted into its dual \mathcal{P}^* by locating the centers of the faces of \mathcal{P}^* at the vertices of \mathcal{P} and the vertices of \mathcal{P}^* above the centers of the faces of \mathcal{P} . Two vertices in the dual \mathcal{P}^* are connected by an edge when the corresponding faces in \mathcal{P} share an edge.

The process of dualization has the following properties:

- (1) The numbers of vertices and edges in a pair of dual polyhedra \mathcal{P} and \mathcal{P}^* satisfy the relationships $v^* = f$, $e^* = e$, $f^* = v$, in which the starred variables refer to the dual polyhedron \mathcal{P}^* . Thus for the octahedron (\mathcal{P})/cube(\mathcal{P}^*) dual pair depicted in Figure 1.1 $v = f^* = 6$, $e^* = e = 12$, $f = v^* = 8$.
- (2) Dual polyhedra have the same symmetry elements and thus belong to the same symmetry point group. Thus in the example above both the octahedron and the cube have the O_h symmetry point group. Also note in general that the dualization of a prism gives the corresponding bipyramid and vice versa.
- (3) Dualization of the dual of the polyhedron leads to the original polyhedron.
- (4) The degrees of the vertices of a polyhedron correspond to the number of edges in the corresponding face polygons in its dual.

The process of dualization can be illustrated by the regular polyhedra (Figure 1.1). Thus the octahedron and cube are dual to each other as are the icosahedron and dodecahedron. The tetrahedron is self-dual.

The problem of the classification and enumeration of polyhedra is a complicated one. Thus there appear to be no formulas, direct or recursive, for which the number of combinatorially distinct polyhedra having a given number of vertices, edges, faces, or any given combination of these elements can be calculated [29,30]. Duijvestijn and Federico have enumerated by computer the polyhedra having up to 22 edges according to the numbers of vertices, edges, and faces and their symmetry groups and present a summary of their methods, results, and literature references to previous work [31]. Their work shows that there are 1, 2, 7, 34, 257, 2606, and 32,300 topologically distinct polyhedra having 4, 5, 6, 7, 8, 9, and 10 faces or vertices, respectively. Tabulations are available for all 301 ($= 1 + 2 + 7 + 34 + 257$) topologically distinct polyhedra having eight or fewer faces [32] or eight or fewer vertices [33]. These two tabulations are essentially equivalent by the dualization relationship discussed above.

In coordination chemistry, the polyhedra of greatest significance in coordination chemistry are those that can be formed by the nine orbitals of the sp^3d^5 valence orbital manifold accessible to d-block transition metals. There are, however, some polyhedra having fewer than nine vertices that cannot be formed by these nine orbitals; such polyhedra are called *forbidden polyhedra* [34,35]. Group theoretical arguments show that polyhedra of the following types are always forbidden polyhedra:

- (1) Polyhedra having eight vertices, a direct product symmetry group $R \times C_s$ or $R \times C_i$ (R contains only *proper* rotations) and the plane in C_s fixing either 0 or 6 vertices.
- (2) Polyhedra having a six-fold or higher C_n rotation axis.

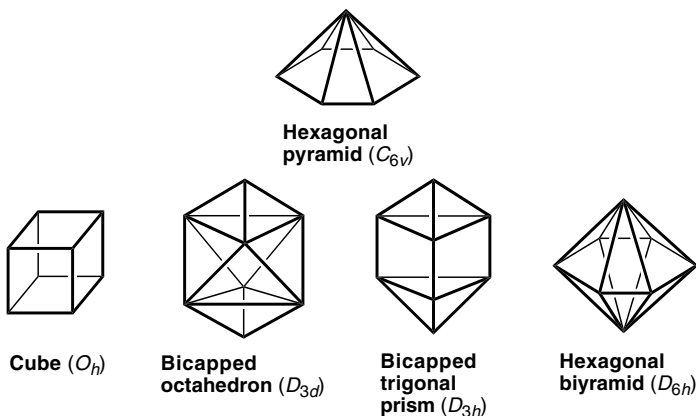


Figure 1.3 Chemically significant forbidden polyhedra: (a) the hexagonal pyramid; (b) examples of eight-vertex polyhedra (all with inversion centers) which cannot be formed from a nine-orbital sp^3d^5 manifold.

Chemically significant forbidden polyhedra include the seven-vertex hexagonal bipyramid and the eight-vertex cube, D_{3d} bicapped octahedron, D_{3h} 3,3-bicapped trigonal prism, and hexagonal bipyramid (Figure 1.3).

In the chemistry of polyhedral boranes and related compounds including their organometallic derivatives, the polyhedra of greatest importance are deltahedra, i.e., polyhedra in which all faces are triangles. Among the large number of such possible deltahedra, the most important deltahedra are the so-called ‘most spherical’ deltahedra, i.e., those where the vertex degrees are as similar as possible to each other. In terms of the structures of the deltahedral boranes $B_nH_n^{2-}$, this means deltahedra having from six to 12 vertices in which all of the vertices are of degree 4 or degree 5 (Figure 1.4).

3 POLYHEDRAL ISOMERIZATIONS: MICROSCOPIC MODELS

3.1 DIAMOND–SQUARE–DIAMOND PROCESSES

A polyhedral isomerization can be defined as a deformation of a specific polyhedron \mathcal{P}_1 until its vertices define a new polyhedron \mathcal{P}_2 . Of particular interest are sequences of two polyhedral isomerization steps $\mathcal{P}_1 \rightarrow \mathcal{P}_2 \rightarrow \mathcal{P}_3$ in which the final polyhedron \mathcal{P}_3 is combinatorially (i.e., topologically) equivalent to the initial polyhedron \mathcal{P}_1 although with some permutation of its vertices, generally not the identity permutation. In this sense two polyhedra \mathcal{P}_1 and \mathcal{P}_3 may be considered to be combinatorially equivalent [36] when there are three one-to-one mappings \mathcal{V} , \mathcal{E} , and \mathcal{F} from the vertex, edge, and face sets, respectively, of \mathcal{P}_1 to

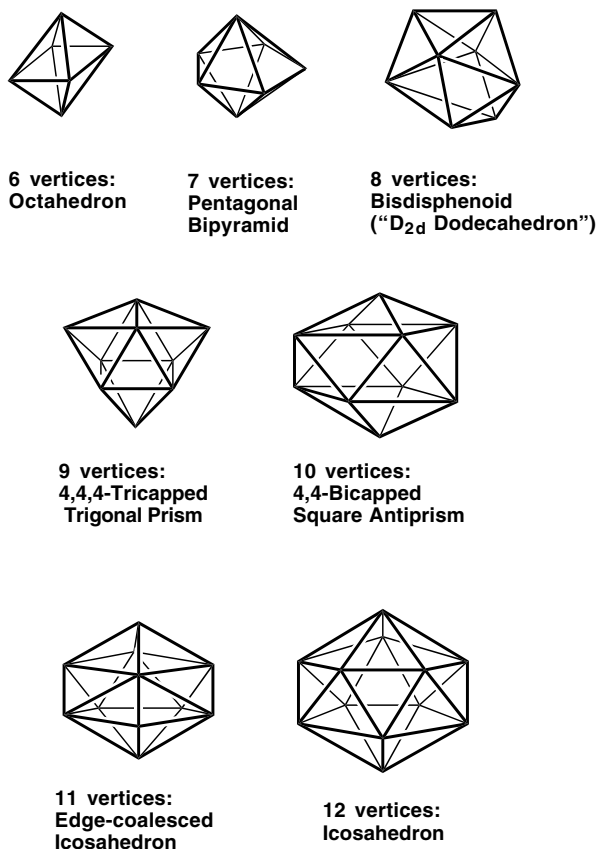


Figure 1.4 The deltahedra found in the boranes $B_nH_n^{2-}$ and isoelectronic carboranes ($6 \leq n \leq 12$).

the corresponding sets of \mathcal{P}_3 such that incidence relations are preserved. Thus if a vertex, edge, or face α of \mathcal{P}_1 is incident to or touches upon a vertex, edge, or face β of \mathcal{P}_1 , then the images of α and β under \mathcal{V} , \mathcal{E} , or \mathcal{F} are incident in \mathcal{P}_3 .

Consider a polyhedral isomerization sequence $\mathcal{P}_1 \rightarrow \mathcal{P}_2 \rightarrow \mathcal{P}_3$ in which \mathcal{P}_1 and \mathcal{P}_3 are combinatorially equivalent. Such a polyhedral isomerization sequence may be called a degenerate polyhedral isomerization with \mathcal{P}_2 as the intermediate polyhedron. Structures undergoing such degenerate polyhedral isomerization processes are often called fluxional [37]. A degenerate polyhedral isomerization with a planar intermediate ‘polyhedron’ (actually a polygon) may be called a planar polyhedral isomerization. The simplest example of a planar polyhedral isomerization is the interconversion of two enantiomeric tetrahedra

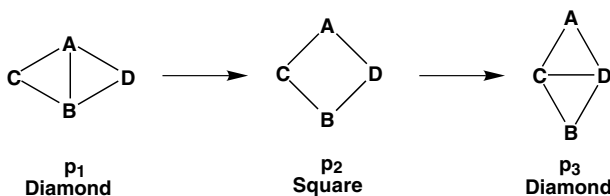


Figure 1.5 The effect of a diamond–square–diamond (dsd) process on a pair of triangular faces sharing an edge.

(\mathcal{P}_1 and \mathcal{P}_3) through a square planar intermediate \mathcal{P}_2 . Except for this simplest example, planar polyhedral isomerizations are unfavorable owing to excessive intervertex repulsion.

Microscopic approaches to polyhedral isomerizations dissect such processes into elementary steps. The most important elementary step is the diamond–square–diamond process that was first recognized in a chemical context by Lipscomb in 1966 [38] as a generalization of a process proposed earlier by Berry [39] for the degenerate isomerization of a trigonal bipyramid. Such a diamond–square–diamond process or ‘dsd process’ in a polyhedron occurs at two triangular faces sharing an edge (Figure 1.5). Thus a configuration such as \mathbf{p}_1 can be called a *dsd situation* and the edge AB can be called a switching edge.

Let a , b , c , and d represent the degrees of the vertices A , B , C , and D , respectively, in \mathbf{p}_1 , then the *dsd type* of the switching edge AB can be represented as $ab(cd)$. In this designation the first two digits refer to the degrees of the vertices joined by AB but contained in the faces (triangles) having AB as the common edge (i.e., C and D in \mathbf{p}_1). The quadrilateral face formed in structure \mathbf{p}_2 may be called a *pivot face*. If a , b , c , and d are the degrees of vertices A , B , C , and D , respectively, in the original diamond (\mathbf{p}_1), then the requirement for a degenerate dsd process is the following:

$$c = a - 1 \quad \text{and} \quad d = b - 1 \quad \text{or} \quad c = b - 1 \quad \text{and} \quad d = a - 1 \quad (1.10)$$

A polyhedron with e edges has e distinct dsd situations; if at least one of these dsd situations is degenerate by satisfying Equation (1.10), then the polyhedron is inherently fluxional [40]. The inherent rigidity/fluxionality of the most important deltahedra including the most spherical deltahedra found in boranes (Figure 1.4) is summarized in Table 1.1.

This simple analysis indicates that in deltahedral structures the 4, 6, 10, and 12 vertex structures are inherently rigid; the 5, 8, 9, and 11 vertex structures are inherently fluxional; and the rigidity of the seven-vertex structure depends upon the energy difference between the two most symmetrical seven-vertex deltahedra [40]. From the point of view of coordination chemistry, note that the trigonal bipyramid and bisdisphenoid, which are favored coordination polyhedra for

Table 1.1 Inherent fluxionality/rigidity of deltahedra

Vertices	Deltahedron	Inherently rigid or fluxional
4	Tetrahedron	Rigid
5	Trigonal bipyramid	Fluxional
6	Octahedron	Rigid
7	Pentagonal bipyramid/ Capped octahedron	$ML_7 \rightarrow$ Fluxional Boranes \rightarrow Rigid
8	Bisdisphenoid	Fluxional
9	Tricapped trigonal prism	Fluxional
10	Bicapped square antiprism	Rigid
11	Edge-coalesced icosahedron	Fluxional
12	Icosahedron	Rigid

coordination numbers 5 and 8, respectively, are inherently fluxional whereas the octahedron found in six-coordinate complexes is inherently rigid. This relates to the stereochemical non-rigidity of five- and eight-coordinate complexes observed experimentally in contrast to the relative rigidity of six-coordinate complexes. In the case of deltahedral borane chemistry, experimental fluxionality observations by boron-11 nuclear magnetic resonance on $B_nH_n^{2-}$ ($6 \leq n \leq 12$) indicate the 6-, 7-, 9-, 10-, and 12-vertex structures to be rigid and the 8- and 11-vertex structures to be fluxional. The only discrepancy between such experiments and these very simple topological criteria for fluxionality in the deltahedral boranes arises in the nine-vertex structure $B_9H_9^{2-}$.

The discrepancy between the predictions of this simple topological approach and experiment for $B_9H_9^{2-}$ has led to the search for more detailed criteria for the rigidity of deltahedral boranes. In this connection Gimarc and Ott have studied orbital symmetry methods, particularly for the five-[41], seven-[42], and nine-[43] vertex borane and carborane structures. A topologically feasible dsd process is orbitally forbidden if crossing of occupied and vacant molecular orbitals (i.e., a ‘HOMO–LUMO crossing’) occurs during the dsd process as illustrated in Figure 1.6 for the single dsd process for the trigonal bipyramid, namely the so-called Berry pseudorotation [39,44]. For such an orbitally forbidden process the activation barrier separating initial and final structures is likely to be large enough to prevent this polyhedral isomerization. However, the forbidden dsd polyhedral rearrangement for the five-vertex $B_5H_5^{2-}$ and corresponding carboranes is allowed in ML_5 coordination compounds and has been observed in PX_5 derivatives such as PCl_5 and PF_5 (i.e., the single fluorine-19 resonance in PF_5) as well as $Fe(CO)_5$ (i.e., the single carbon-13 or oxygen-17 resonance). Guggenberger and Muetterties [45] point out that cage framework rearrangements such as those in the deltahedral boranes and carboranes involve bond stretches which must require more energy than bond angle changes that occur in coordination polyhedra of ligands bound to a central atom.

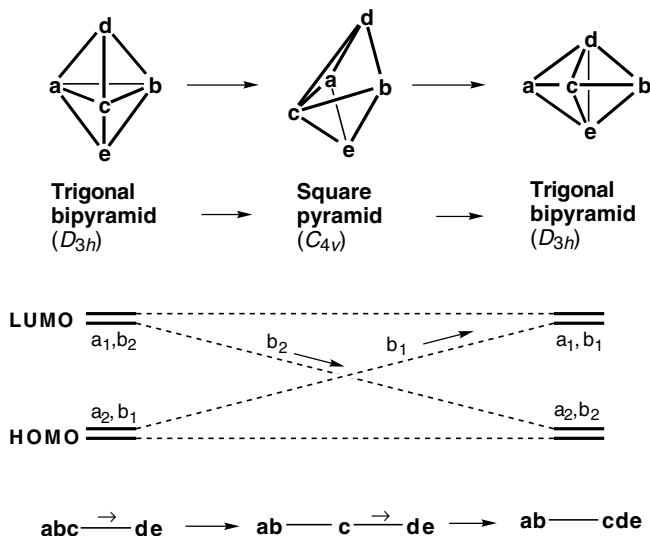


Figure 1.6 (a) The single dsd process converting a trigonal bipyramid to an isomeric trigonal bipyramid through a square pyramid intermediate (Berry pseudorotation). (b) The orbital crossing for this dsd process. (c) Gale diagrams for this polyhedral isomerization sequence.

Some selection rules have been proposed for distinguishing between symmetry-allowed and symmetry-forbidden processes in deltahedral boranes, carboranes, and related structures. Thus Wales and Stone [46] distinguish between symmetry-allowed and symmetry-forbidden processes by observing that a HOMO–LUMO crossing occurs if the proposed transition state has a single atom lying on a principal C_n rotational axis where $n \geq 3$. A more detailed selection rule was observed by Mingos and Johnston [47]. If the four outer edges of the two fused triangular faces (i.e., the ‘diamond’) are symmetry equivalent, then a single dsd process results in a pseudorotation of the initial polyhedron by 90° (Figure 1.7a) such as occurs for the trigonal bipyramid in Figure 1.6. However, if the edges are not symmetry equivalent (as indicated by the regular and bold edges in Figure 1.7b), then the rearrangement results in a pseudoreflexion of the initial polyhedron. Pseudorotations are symmetry forbidden and have larger activation energies than pseudoreflexions, which are symmetry allowed. Subsequent work by Wales *et al.* [48] has shown that a dsd process in which a mirror plane is retained throughout involves an orbital crossing and is therefore symmetry forbidden in accord with the earlier work by Gimarc and Ott [41].

The fact that a degenerate single dsd isomerization of the D_{3h} nine-vertex tricapped trigonal prismatic $B_9H_9^{2-}$ through a C_{4v} capped square antiprismatic intermediate (Figure 1.8a) is orbitally forbidden [43] has stimulated searches

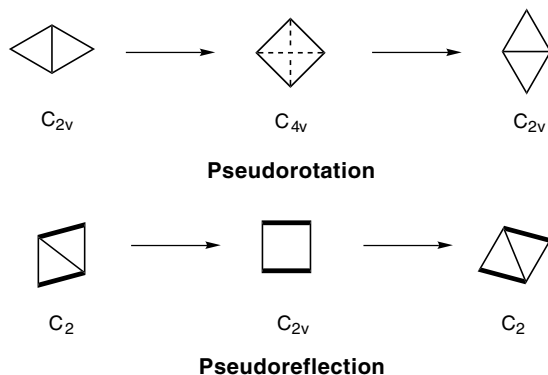


Figure 1.7 (a) A pseudorotation process involving an intermediate with a C_4 axis. (b) A pseudoreflexion process involving an intermediate without a C_4 axis.

for other isomerization mechanisms for the tricapped trigonal prism. In this connection Gimarc and Ott [43] have found a double dsd isomerization of $B_9H_9^{2-}$ (Figure 1.8b) to be orbitally allowed. However, Ceulemans *et al.* [49] have shown by computation that an analogous double dsd isomerization of the carborane $C_2B_7H_9$ passes through an intermediate with an open hexagonal face thereby preserving C_{3v} subgroup symmetry of the D_{3h} point group of the original tricapped trigonal prism.

3.2 GALE DIAGRAMS

Gale diagrams provide an elegant mathematical method for the study of microscopic aspects of rearrangement of polyhedra having relatively few vertices (i.e., for $v \leq 6$) by reducing the dimensionality of the allowed vertex motions. In a chemical context Gale diagrams can be used to study possible rearrangements of six-atom structures. Using this approach the skeletal rearrangements of the six atoms are depicted as movements of six points on the circumference of a circle or from the circumference to the center of the circle subject to severe restrictions that reduce possible such movements to a manageable number [50].

Consider a polytope \mathcal{P} in d -dimensional space \mathbb{R}^d , where the term ‘polytope’ refers to the generalization of the concept of ‘polyhedron’ to any number of dimensions [36]. The minimum number of vertices of such a polytope is $d + 1$ and there is only one such polytope, namely the d -simplex in which each possible pair of the $d + 1$ vertices are connected by an edge corresponding to the so-called complete graph [51] K_{d+1} . The combinatorially distinct possibilities for d -dimensional polytopes having only $d + 2$ and $d + 3$ vertices (polyhedra with ‘few’ vertices) are also rather limited. They can be represented faithfully in a space of less than d dimensions through a Gale

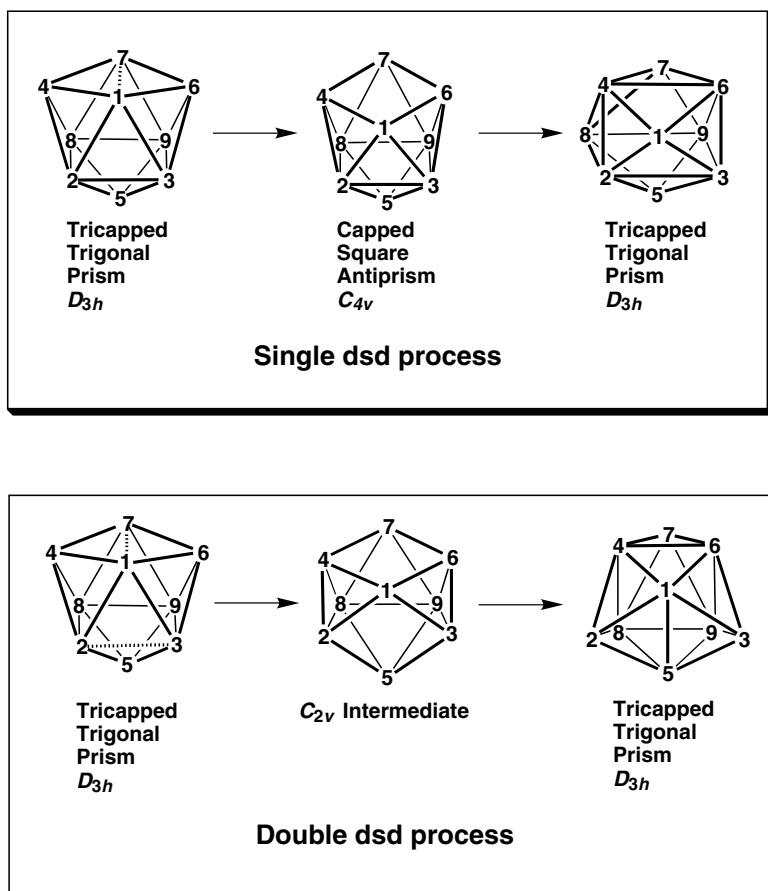


Figure 1.8 (a) A forbidden single dsd degenerate isomerization of a tricapped trigonal prism. (b) An allowed double dsd degenerate isomerization of a tricapped trigonal prism.

transformation [52]. More specifically, if \mathcal{P} is a d -dimensional polytope with v vertices, a Gale transformation leads to a Gale diagram of \mathcal{P} consisting of v points in $(v-d-1)$ -dimensional space \mathbb{R}^{d-1} in one-to-one correspondence with the vertices of \mathcal{P} . From the Gale diagram it is possible to determine all of the combinatorial properties of \mathcal{P} such as the subsets of the vertices of \mathcal{P} that define faces of \mathcal{P} , the combinatorial types of these faces, etc. The combinatorial properties of a polytope \mathcal{P} which can be determined by the Gale diagram include all possible isomerizations (rearrangements) of \mathcal{P} to other polytopes having the same number of vertices and imbedded in the same number of dimensions as \mathcal{P} . Also of particular importance is the fact that, if v is not much larger than d (i.e., if $v \leq 2d$), then the dimension of the Gale diagram is smaller than that of the original polytope \mathcal{P} .